Computational and Theoretical Chemistry 972 (2011) 32–38

Contents lists available at ScienceDirect

Computational and Theoretical Chemistry

journal homepage: www.elsevier.com/locate/comptc

A study of TDDFT performance in modeling of spectral changes induced by interactions of ketocyanine dyes with inorganic ions

Andrzej Eilmes *

Department of Computational Methods in Chemistry, Jagiellonian University, Ingardena 3, 30-060 Kraków, Poland

ARTICLE INFO

Article history:
Received 23 May 2011
Received in revised form 15 June 2011
Accepted 15 June 2011
Available online 21 June 2011

Keywords:
TDDFT
Ion complexation
Ketocyanine dyes
Spectral shifts
DFT functionals performance

ABSTRACT

DFT/TDDFT calculations were conducted for series of ketocyanine dye complexes with inorganic cations in acetonitrile and acetone. Four functionals were investigated: B3LYP, CAM-B3LYP, LC-PBE and wB97XD. Franck–Condon vibrational analysis was performed to simulate the shape of absorption and emission spectra. Results of computations were compared with available experimental data. The best reproduction of the positions of maxima in absorption and emission spectra was obtained for B3LYP. wB97XD and CAM-B3LYP performed better in the prediction of complexation-induced spectral shifts.

1. Introduction

It is well known that spectral properties of organic dyes are affected by dye interactions with the solvent. Even more pronounced changes in absorption or emission spectra are induced when a complex between dye molecule and an inorganic cation is formed. Ketocyanine dyes are an example of a class of dyes with solvent-dependent spectral properties and sensitivity to interactions with ions [1], therefore these compounds are good probes for studying microenvironmental effects in electrolyte solutions. In recent years absorption and fluorescence spectra of ketocyanine dyes in salt solutions in organic solvents were studied experimentally [1–5] revealing substantial complexation-induced red shifts.

One of the most popular methods in theoretical investigations of excited states is Time Dependent Density Functional Theory (TDDFT) owing to its relatively low computational cost, good performance for organic systems and widespread availability in popular quantum-chemical software. Numerous works focused on the assessment of performance of different functionals (e.g. long-range-corrected functionals used to study organic dyes [6–10]) or modeling of solvent effects.

There are a few examples of TDDFT methodology applied to study excited states in the complexes of organic molecules with inorganic ions, e.g. complexation of flavonoids with iron [11] or copper [12], complexation of organic dyes with divalent metal cations [13,14], TDDFT investigations of Maya Blue [15] or a study of crown ether complexes with divalent cations [16]. Recently a DFT/TDDFT study on ketocyanine dye complexes with lithium and magnesium ions in acetonitrile was performed [17]. Calculations of such kind were also reported for ketocyanine dye interactions with cobalt ions [18]. Explicit solvent model and the effect of counterions were studied in TDDFT calculations for a ketocyanine dye–ion system in acetonitrile [19].

Development of the quantum-chemical software and steady increase in the performance of the hardware facilitates calculations for systems of increasing size and brings more time-demanding methodology (e.g. vibrational analysis) into routine use. However, with broad choice of functionals which may be used in TDDFT computations, assessment of their performance for different systems becomes even more desirable.

Quite large amount of spectroscopic data available for ketocyanine dyes in electrolyte solutions, covering a range of dyes, cations, and solvents [1–5] make these systems well suited to study the applicability of TDDFT methodology and different functionals to dye–ion complexes. In this paper we attempt to explore this opportunity. Availability of excited state gradients allows for the calculations of excited state vibrational frequencies and Franck–Condon vibrational analysis provides a tool for simulating the shape of absorption or emission spectra, which may be directly compared with experimental data. We performed therefore such calculations for a series of systems, testing different DFT functionals. In particular we attempted to check whether the functionals with long-range corrections improve agreement between calculated and measured transition energies and whether they help to reduce problems with spurious states encountered in earlier work [17]. In following sections we describe model systems and details of cal-

* Tel.: +48 12 6632030; fax: +48 12 6340515.
E-mail address: eilmes@chemia.uj.edu.pl

2210-271X/$ - see front matter © 2011 Elsevier B.V. All rights reserved.
doi:10.1016/j.comptc.2011.06.009

culations and then we present the results of spectra simulations compared with the data available in the literature.

2. Methodology and calculations

2.1. Model systems

In this work we studied three ketocyanine dyes investigated experimentally [1–5] shown in Fig. 1. Thorough the paper we will refer to them as to dye A, B, and C. Two monovalent (Li^+, Na^+) and two divalent (Mg^{2+}, Ca^{2+}) cations were used as complexing ions. Two aprotic solvents were commonly used in experiments with ketocyanines: acetonitrile (ACN) and acetone (AC). Accordingly, we performed calculations for all combinations of above dyes, ions and solvents for which experimental data are available in the literature, i.e. Li^+ and Mg^{2+} with dye A in ACN, Li^+ and Mg^{2+} with dye B in ACN or AC, all four cations with dye C in ACN and Li^+, Na^+ and Mg^{2+} with dye C in AC.

2.2. Methodology

Gaussian 09 Rev. A02 [20] was used in all quantum-chemical calculations in this work. In [17] it has been found that the best reproduction of spectral shifts for Li^+ and Mg^{2+} complexes of dye A in ACN was obtained for hybrid functionals, especially B3LYP and O3LYP. Accordingly we used B3LYP in the present study. Three other functionals with long-range correction were also tested: CAM-B3LYP [21], LC-PBE (PBE with LC correction [22]) and wB97XD [23] from the wB97 family; the latter contains also the empirical dispersion correction. In the case of LC-PBE, Gaussian 09 default value $\omega = 0.47$ was used for the damping parameter controlling the growth rate of the exact exchange with increasing distance.

Both solvents (acetonitrile and acetone) were modeled by Polarizable Continuum Model (PCM). Universal Force Field atomic radii and van der Waals surface were used to construct the molecular cavity in the solvent (Gaussian 09 default). In principle, one might perform TDDFT calculations with different PCM cavity parameterizations to determine which one gives the best agreement with experimental data. This would, however, significantly increase the computational effort. Instead, informed by model studies comparing explicit and implicit solvent models [19,24] we choose the default parameterization. As we will show later, this radii/surface combination leads to the parentage of observable transitions in agreement with explicit solvation modeling of dye A/Li^+ and dye A/Mg^{2+} spectra in acetonitrile [19]. This cavity parameterization was also among the best performing in an explicit/implicit solvent study of Li^+ complexation energies in ACN [24] which further supports the choice made in this work. Default Gaussian 09 values of dielectric permittivity were used (ACN: 35.7 and 1.81; AC: 20.5 and 1.85 for static permittivity and the permittivity at infinite frequency, respectively).

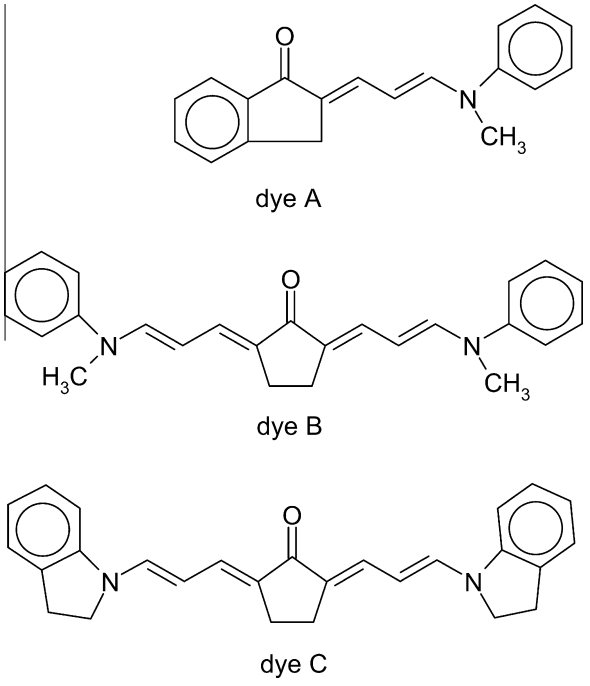

Fig. 1. Ketocyanine dyes studied in this work.

For each density functional optimizations of the geometry and calculations of vibrational frequencies in the ground state for all dyes and dye/cation complexes were performed in the 6-31G(d, p) basis set followed by the linear response TDDFT calculations of transition energies to five lowest excited states. Then the geometry of the system in the first excited state was optimized and the excited state vibrational modes were obtained at the 6-31G(d, p) level. Resulting structures of complexes and harmonic frequencies were then used in the Franck–Condon vibrational analysis implemented in Gaussian 09 [25,26] to compute the shape of simulated absorption and emission spectra. Bandwidth of 1000 cm^{-1} was used in spectra calculations; this value yielded broad bands with no noticeable vibrational structure in agreement with the shape of experimental spectra [1–5].

In earlier study on ketocyanine dye complexes it has been found that in the B3LYP/TDDFT calculations vertical energies calculated in aug-cc-pVDZ and in aug-cc-pVTZ basis set differ by less than 2 nm [17]. In this work we performed similar test for long-range-corrected CAM-B3LYP functional. For dye A and its complexes with Li^+ or Mg^{2+} in ACN the differences between double and triple zeta basis were smaller than 1 nm, i.e. lower than accuracy of experimental values. Therefore we concluded that aug-cc-pVDZ basis provides satisfactory accuracy in calculations of transition energies.

Single-point energy and TDDFT calculations in the aug-cc-pVDZ basis (or 6-31++G(d, p) for Ca^{2+}) were performed to find the energies of the ground and the first excited state at the geometries optimized in smaller basis set. Energy differences between the potential energy minima of the ground and the excited state were then used to shift the spectra calculated from 6-31G(d, p) data to the energies corresponding to aug-cc-pVDZ excitations (similar procedure, but without frequency calculations was used to obtain energies of vertical transitions and relaxation energies of excited states in [17]). This shift accounts not only for the basis set difference but also for the non-equilibrium solvation effect. In the PCM methodology geometry optimizations are performed within equilibrium solvation, because the solvent has enough time to respond to the changes of solute geometry. On the other hand, excitation of the molecule occurs on much shorter timescale and non-equilibrium solvation is more relevant to calculations of vertical transition energies [27]. Therefore, performing vibrational analysis for the energy difference between the ground state minimum (optimized within equlibrium solvation) and the minimum of excited state obtained from non-equlibrium solvation TD calculations (as resulted from our aug-cc-pVDZ correction) seems more appropriate than simply using the energy difference between the ground and excited state minima calculated within equilibrium scheme.

3. Results

3.1. Complexation energies

From the values of total energy for optimized structures one can obtain information about the strength of dye–ion interactions in

Table 1
Complexation energies (in kcal/mol) for ketocyanine dyes in the ground and in the excited state calculated within the PCM approach at the 6-31G(d, p) level.

Dye–ion/solvent	B3LYP		CAM-B3LYP		LC-PBE		wB97XD	
	Ground	Excited	Ground	Excited	Ground	Excited	Ground	Excited
A-Li^+/ACN	−12.7	−16.8	−13.0	−18.7	−10.4	−17.1	−9.6	−14.4
A-Mg^{2+}/ACN	−30.4	−36.9	−31.0	−40.0	−26.8	−38.7	−23.2	−32.4
B-Li^+/ACN	−14.6	−19.5	−14.6	−22.3	−11.6	−21.0	−10.5	−17.2
B-Mg^{2+}/ACN	−34.5	−42.7	−34.4	−47.4	−29.5	−46.8	−26.3	−38.5
B-Li^+/AC	−15.9	−21.0	−15.8	−23.8	−12.7	−22.5	−11.6	−18.7
B-Mg^{2+}/AC	−37.4	−46.5	−37.0	−50.7	−32.0	−50.0	−28.8	−41.9
C-Na^+/ACN	−11.7	−15.2	−12.0	−17.4	−9.8	−16.3	−9.1	−13.7
C-Li^+/ACN	−14.8	−19.7	−14.7	−22.3	−11.6	−20.9	−10.5	−17.2
C-Ca^{2+}/ACN	−17.8	−23.5	−17.9	−26.8	−15.4	−26.9	−14.6	−23.0
C-Mg^{2+}/ACN	−34.9	−43.2	−34.5	−48.2	−29.5	−46.9	−26.2	−38.7
C-Na^+/AC	−12.6	−16.3	−12.9	−18.6	−10.6	−17.5	−9.9	−14.9
C-Li^+/AC	−16.0	−21.2	−15.9	−23.9	−12.7	−22.4	−11.6	−18.7
C-Mg^{2+}/AC	−37.7	−46.4	−37.1	−50.9	−31.9	−50.0	−28.7	−41.8

the ground and in the excited state of the complex. The cation complexation energies ΔE^{gr} and ΔE^{ex} were calculated as:

$$\Delta E^{st} = E_c^{st} - (E_{ion} + E_{dye}^{st}), \quad st = gr,\ ex$$

where E_c^{st} and E_{dye}^{st} stand for the energies of the dye–ion complex and the dye molecule in the ground ($st = gr$) or in the excited ($st = ex$) state and E_{ion} is the energy of a free cation. All energies were taken from the PCM calculations, therefore they contain electrostatic corrections due to the implicit solvent.

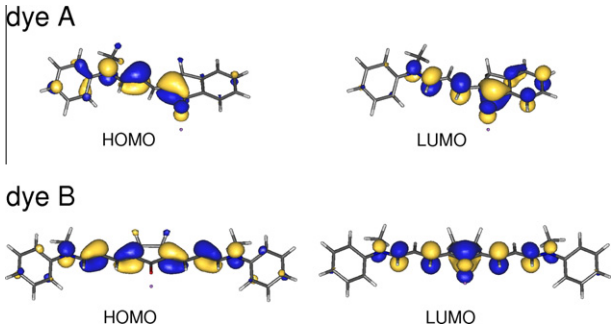

Fig. 2. Plots of HOMO and LUMO for Li^+ complexes with dyes A and B in acetonitrile obtained from B3LYP/aug-cc-pVDZ calculations at the B3LYP/6-31G(d, p) geometries.

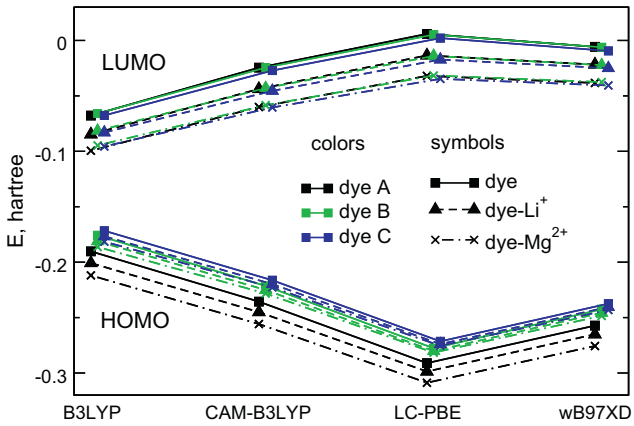

Fig. 3. HOMO and LUMO energies for dyes A–C and their complexes with Li^+ and Mg^{2+} calculated at the 6-31G(d, p) level in ACN. Lines are only to guide the eye; slight horizontal shift was applied to the data to improve readability. Colors mark different dyes and symbols different ions. (For interpretation of the references to color in this figure legend, the reader is referred to the web version of this article.)

Although in principle it is possible to apply the counterpoise correction for Basis Set Superposition Error in solvent calculations [28], this is not a straightforward procedure. Therefore to estimate the size of the BSSE we performed for selected complexes of dyes A and C test calculations of the counterpoise correction to complexation energy in 6-31G(d, p) basis in vaccum at the geometry of the complex obtained from the PCM calculations. Counterpoise corrections are between 2.5–4.1 kcal/mol, the largest are the values for B3LYP and CAM-B3LYP functionals and the smallest for wB97XD (Table S1 in Supplementary material). Taking the vacuum counterpoise corrections as the estimate of the BSSE in the solvent we can conclude that they do not change ordering of calculated complexation energies.

Calculated values of (BSSE-uncorrected) complexation energies are collected in Table 1. B3LYP values for dye A/Li^+, Mg^{2+}/ACN differ from the results reported in [17], because in the present work different parameterization of the PCM cavity was used; according to

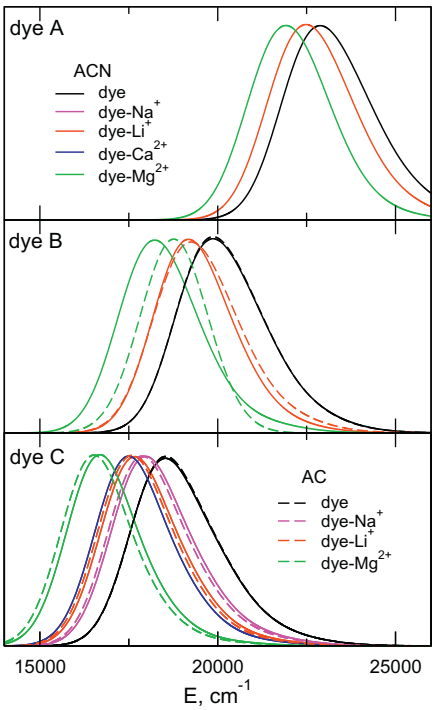

Fig. 4. Absorption spectra for complexes of dyes A–C in ACN and AC obtained from vibrational analysis of the B3LYP/6-31G(d, p) data shifted to aug-cc-pVDZ energies. Solid lines – ACN, dashed lines – AC. Spectra were rescaled to the same height.

Table 2
Experimental and calculated values (in cm^{-1}) of the maxima in the absorption and the emission spectra for ketocyanine dyes and dye complexes with ions (upper rows) and the spectral shifts with respect to free dye (bottom rows for dye/ion complexes). Results of vibrational analysis of 6-31G(d, p) data were shifted to aug-cc-pVDZ transition energies. For each experimental data category (except for dye C/Na^+/AC) the best calculated value is typed in boldface and the worst in italics.

Dye/ion/solvent	Experiment		B3LYP		CAM-B3LYP		LC-PBE		wB97XD	
	Abs.	Em.	Abs.	Em.	Abs.	Em.	Abs.	Em.	Abs.	Em.
A/ACN[a]	23,529	20,202	**22,882**	**21,697**	25,952	24,314	*28,905*	*25,424*	26,145	24,437
A/Li^+/ACN[a]	22,727	19,608	**22,485**	**21,050**	24,852	23,477	*26,989*	*24,853*	25,320	23,692
	−802	−594	−397	−647	−1100	*−837*	*−1916*	**−571**	**−825**	−745
A/Mg^{2+}/ACN[a]	21,277	19,048	**21,919**	**20,258**	23,926	22,462	*25,431*	*23,716*	24,943	22,076
	−2253	−1154	*−963*	**−1439**	**−2026**	−1852	−3474	−1708	−1202	*−2361*
B/ACN[b]	21,053	18,519	**19,868**	**18,785**	23,057	21,562	*26,179*	*23,275*	23,343	21,902
B/Li^+/ACN[b]	19,417	17,699	**19,181**	**18,072**	22,013	20,338	*24,532*	*21,819*	22,264	20,788
	−1635	−819	*−687*	**−713**	−1044	−1224	**−1647**	*−1456*	−1079	−1114
B/Mg^{2+}/ACN[c]	18,519	16,807	**18,228**	**17,200**	20,162	18,915	*21,565*	*19,752*	20,784	18,644
	−2534	−1712	−1640	**−1585**	−2895	−2647	*−4614*	*−3523*	**−2559**	−3258
B/AC[b]	21,277	19,048	**19,870**	**18,789**	23,081	21,608	*26,229*	*23,394*	23,320	21,908
B/Li^+/AC[b]	19,802	18,018	**19,253**	**18,014**	21,861	20,293	*24,384*	*21,766*	21,114	19,694
	−1475	−1030	−617	**−775**	**−1220**	−1315	−1844	−1627	*−2206*	*−2214*
B/Mg^{2+}/AC[c]	18,692	17,094	**18,764**	**16,135**	19,757	18,770	*21,445*	*19,864*	20,180	18,606
	−2585	−1954	−1106	**−2654**	−3324	−2838	*−4784*	*−3530*	**−3140**	−3302
C/ACN[c]	19,881	17,699	**18,530**	**17,849**	21,905	20,648	*25,226*	*22,332*	22,308	21,080
C/Na^+/ACN[d]	19,048	17,094	**17,975**	**17,353**	20,945	19,776	*24,046*	*21,619*	21,366	20,356
	−833	−605	−555	−496	−961	*−873*	*−1180*	**−713**	**−942**	−724
C/Li^+/ACN[d,e]	18,519	16,529	**17,669**	**17,075**	20,452	19,325	*23,485*	*21,018*	21,112	19,881
	−1362	−1170	*−861*	*−774*	**−1453**	−1323	−1741	−1314	−1196	**−1199**
C/Ca^{2+}/ACN[c,f]	17,544	16,000	**17,496**	**16,397**	20,142	19,108	*22,976*	*20,812*	20,575	19,645
	−2337	−1699	*−1034*	*−912*	−1764	**−1541**	**−2250**	−1520	−1733	−1435
C/Mg^{2+}/ACN[c]	17,241	15,873	**16,687**	**16,166**	20,220	16,270	*20,561*	*18,618*	19,444	18,530
	−2639	−1826	−1843	**−1683**	−1686	−4379	*−4665*	*−3714*	**−2863**	−2549
C/AC[c,e]	20,202	18,182	**18,541**	**17,866**	21,942	20,697	*25,280*	*22,437*	22,335	21,134
C/Na^+/AC[d]		17,699	17,885	17,282	20,847	19,724	23,914	21,565	21,332	20,345
		−483	−656	−584	−1095	−973	−1366	−872	−1003	−789
C/Li^+/AC[e]	18,868	16,807	**17,586**	**17,000**	20,324	19,244	*23,332*	*20,937*	20,998	19,809
	−1334	−1375	−955	*−866*	−1618	−1453	*−1948*	−1500	**−1337**	**−1325**
C/Mg^{2+}/AC[c]	17,544	16,129	16,523	**16,032**	**18,558**	17,734	*20,429*	*19,001*	19,199	18,310
	−2658	−2053	**−2017**	**−1833**	−3384	−2963	*−4851*	*−3436*	−3136	−2824

[a] Exp. data from Ref. [5].
[b] Exp. data from Ref. [4].
[c] Exp. data from Ref. [1].
[d] Exp. data from Ref. [2].
[e] Exp. data from Ref. [3].
[f] For Ca^{2+} 6-31++G(d, p) basis set was used instead of aug-cc-pVDZ.

the findings of [24] it yields better agreement with explicit solvation model. The strength of dye–ion interaction increases in the order $Na^+ < Li^+ < Ca^{2+} < Mg^{2+}$, as expected from simple reasoning: the electric field of the ion increases with increasing charge and decreasing radius. Likewise, basic arguments explain that stronger cation binding in AC compared to ACN originates from weaker screening of electrostatic interactions in the solvent with lower permittivity. For all cations and solvents the cation-binding ability is weaker for dye A. For dyes B and C the dye–ion interaction is almost the same, which is expectable as the parts of molecules which are different between the two dyes are far away from the ion-binding site (*keto* oxygen atom).

As readily seen from Table 1, the dye–cation interaction is significantly stronger in the excited state. This effect is the most pronounced for the LC-PBE functional for which the largest difference between the ground and excited state amounts to 18 kcal/mol (for Mg^{2+} interaction with dye B or C in AC). The strongest complexation in excited state is obtained for CAM-B3LYP functional and in the ground state for B3LYP and CAM-B3LYP. For both states ion binding is the weakest for wB97XD. For CAM-B3LYP and LC-PBE functionals the long-range correction apparently increases the interaction of the ion with dye molecule in excited state. This is very well noticeable for B3LYP and CAM-B3LYP, where ground state complexation energies are the same (thus not affected by the long-range correction), but the binding strength in the excited state is significantly enhanced for CAM-B3LYP.

The increase of the ion–dye interaction energy in the excited state correlates with the ion – keto oxygen distance (Table S2 in Supplementary material). The ion – O distance in the excited state noticeably decreases; largest changes (up to 0.09–0.1 Å) are observed for wB97XD functional.

3.2. Vertical transitions and frontier orbitals

For all systems the lowest intensity-carrying transition was the first transition and originated from the HOMO → LUMO excitation. This is consistent with findings of Ref. [19] for the dye A and its complexes with Li^+ or Mg^{2+} in acetonitrile modeled as explicit solvent – for sufficiently large number of ACN molecules included in TDDFT calculations the lowest transition is of the HOMO → LUMO parentage and acquires oscillator strength. Therefore, in the context of relation to explicit solvation data, the UFF atomic radii/van der Waals surface combination in PCM calculations performs better than United Atom Kohn–Sham radii/Solvent Excluding Surface used in [17] in which case the observable transition for dye A/Mg^{2+} in ACN was the second transition and originated from HOMO → LUMO + 1 excitation. No spurious states below the first observable transition appeared regardless of the DFT functional used in calculations, therefore it seems that the PCM parameterization used in this work eliminates problems with "ghost" states encountered in [17] with no necessity to use long-range corrections in the functional.

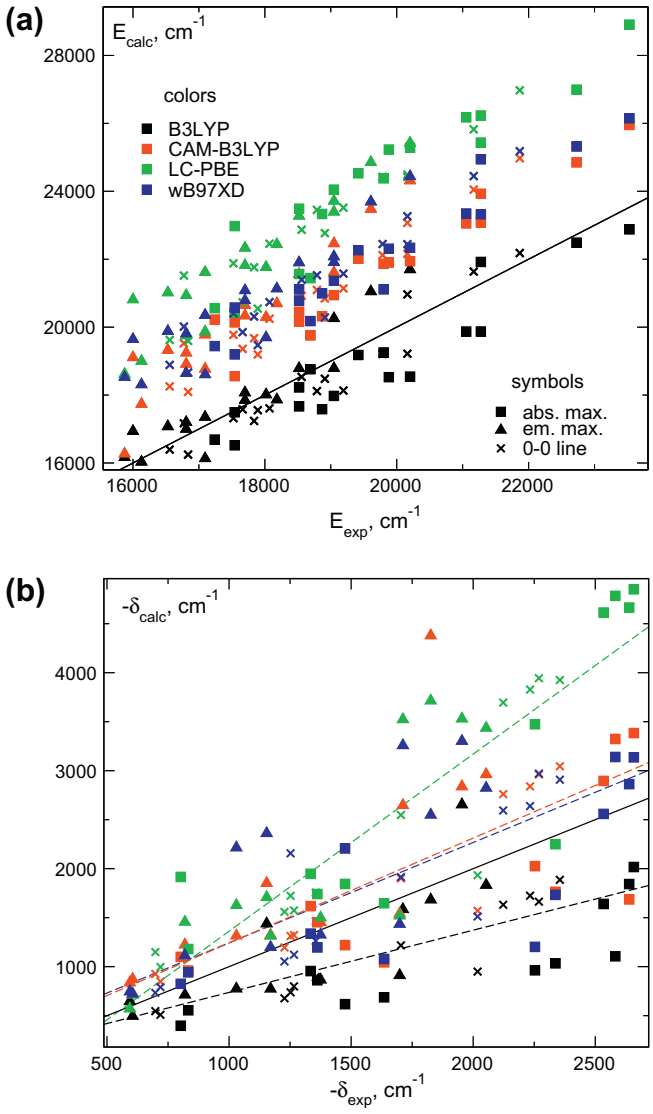

Fig. 5. Correlation between experimental and calculated positions of absorption (squares) and emission (triangles) maxima and 0–0 lines (crosses) (a) and their shifts (b) for ketocyanine dye complexes. Colors mark different functionals. Solid line is the $y = x$ line. Dashed lines in panel (b) are the linear fits to the data sets. (For interpretation of the references to color in this figure legend, the reader is referred to the web version of this article.)

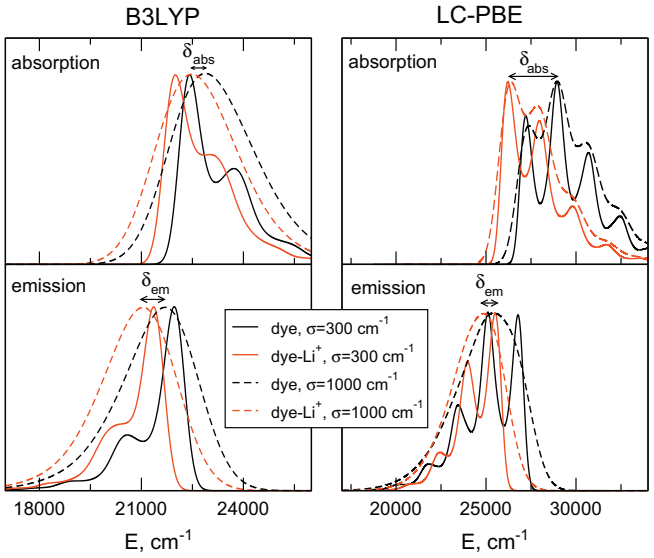

Fig. 6. Absorption and emission spectra calculated for B3LYP and LC-PBE functionals for dye A/Li^+ complex in ACN. Results for two different bandwidths are presented. Note the difference in the energy scale between functionals.

Plots of frontier orbitals obtained from B3LYP calculations for Li^+ complexes with dyes A and B are shown in Fig. 2 (results for CAM-B3LYP functional are the same; more plots are available in Supplementary material). The observable transition apparently corresponds to a $\pi \rightarrow \pi^*$ excitation. The electron density in the LUMO shifts towards the five-membered ring and the C=O group.

Before discussing details of calculated transition energies and simulated spectra it is convenient to present general trends in the pattern of orbitals involved in the transition. In Fig. 3 HOMO and LUMO energies for all four functionals are displayed for dyes A–C and complexes with Li^+ and Mg^{2+} in ACN. The HOMO–LUMO gap is the smallest for B3LYP, increases for functionals with long-range correction and is the largest for LC-PBE. Therefore we should expect that the transition energies in TDDFT will be the smallest for B3LYP and will increase for other functionals, especially for LC-PBE.

HOMO – LUMO separation decreases in the order dye > dye/Li^+ > dye/Mg^{2+} in accord with the observation that ion complexation shifts the transition to lower energy. For given cation the gap is the largest for dye A and the smallest for dye C, which will be reflected in the spectra. It is noticeable that the LUMO energy does not significantly depend on the type of the dye, therefore the changes in the HOMO–LUMO gap arise mainly from the increase of the HOMO energy in the order dye A < dye B < dye C.

3.3. Absorption and emission spectra

Using the procedure described in Section 2.2 simulated absorption and emission spectra were obtained for free dyes and dye–cation complexes. In Fig. 4 absorption spectra obtained with B3LYP functional are presented. In accordance with the values of the HOMO–LUMO gap, the energy of the absorption maximum is the highest for dye A and the smallest for dye C. Cation complexation induces red-shifts in the spectrum which are larger for stronger electric field of the ion. Therefore the shifts increase in the same order as the complexation energies discussed in Section 3.1. Differences between solvents are usually smaller than between different cations; because the dielectric constant at infinite frequency (relevant for the vertical transition energy calculations) is similar, larger differences between ACN and AC occurring for some systems (e.g. dye B/Mg^{2+} in B3LYP) are likely to be caused by slightly different geometry of the complex.

Table 2 collects the experimental [1–5] and calculated positions the absorption or emission maxima. To facilitate comparison of shifts at different energies, linear energy scale is more convenient, therefore values of energy (in cm^{-1}) rather than wavelengths are presented. The 0–0 line position is not directly available from the experimental data, nevertheless it may be useful, because in many cases it averages errors of the absorption and emission maximum. "Experimental" 0–0 line positions were therefore estimated as arithmetic means of the absorption and emission band maxima. Numerical data for 0–0 lines are collected in Table S3 in Supplementary material. For each data category (absorption or emission maximum position or shift) values closest to experiment and the worst results are marked in Table 2.

To visualize the results, Fig. 5 displays calculated positions of 0–0 lines or band maxima and predicted spectral shifts versus experimental values. Clearly, B3LYP outperforms the other three functionals in reproduction of the band maxima and 0–0

line positions. Functionals with long-range corrections give systematically overestimated values, with CAM-B3LYP and wB97XD being very similar (in agreement with the results of Ref. [10]) and LC-PBE always yielding values farthest to the experiment.

For spectral shifts the picture is more complicated – relative errors are much larger than in the case of band positions and in some instances the deviation from the experiment is remarkably large (e.g. emission band maximum for dye C/Mg^{2+} in ACN). The best overall reproduction of band positions for B3LYP does not necessary lead to good values of spectral shifts. Indeed, closer inspection of data in Table 2 reveals that the transition energies for free dyes are usually underestimated in B3LYP calculations while for dye–cation complexes the difference to the experiment is smaller or even changes sign. Therefore, although for the whole series the average error of the band positions for B3LYP calculations is the smallest for all functionals, shift values are too small because errors for free dyes and complexes have systematically opposite signs. Long range-corrected functionals give better reproduction of spectral shifts with the exception of LC-PBE producing usually too high values.

In the experimental data the shift of the absorption maximum is always larger than the shift in the emission spectrum. This feature is reproduced only by LC-PBE and in the case of other functionals it is observed mainly for complexes of dye C. As a consequence, B3LYP sometimes yields the best reproduction of the shift in emission spectrum for dye A or B complexes, but because the ratio between absorption and emission shifts in reversed with respect to the experiment, shifts in the absorption spectra are in such cases seriously underestimated.

To give some insight into the nature of different relative values of absorption and emission shifts for different functionals, in Fig. 6 we compare the B3LYP and LC-PBE results for dye A/Li^+ in ACN. To visualize the vibrational structure of the band, results for smaller bandwidth ($\sigma = 300\ cm^{-1}$) are displayed. For LC-PBE functional the second peak in the spectra of free dye is comparable or even higher that the first one, while in the spectra of the dye – Li^+ complex the first maximum dominates. As a result the dye-to-complex shift in the absorption spectrum is much larger than in the emission. In the case of B3LYP for both systems the first peak is dominant and therefore the spectral shifts in absorption and emission are comparable. This suggests that the predicted ratio of absorption/emission shifts depends on how well calculations within given functional reproduce changes in the geometry of the molecule upon excitation (and the curvature of the potential in the excited state) for free dye and the complex.

There is also another factor, related to the modeling of solvation, which is likely to affect the relative values of absorption and emission shifts in solution. As mentioned in Section 2.2, the solvent effect on transition energies should be modeled by using non-equlibrium solvation in TD calculations of the vertical transition from the potential energy surface of the initial state optimized within equilibrium scheme. The initial state is different for absorption and emission and therefore in principle different values of the energy difference between the two states should be used in calculations of band shape in absorption and emission spectra. This factor, which was not accounted for in calculations, may systematically affect the ratio of absorption and emission shifts for complexed dyes.

From the fits to the data shown in Fig. 5 it is noticeable that B3LYP and LC-PBE give reasonable estimates of the spectral shifts only in the cases, where the experimental shifts are small. For larger shifts the differences with respect to the experiment increase. B3LYP underestimates the effect and LC-PBE leads to its significant overestimation. On the other hand, CAM-B3LYP and xB97DX perform quite well. Moreover, their overestimate of the shift is in average rather constant over the whole data set, which opens the possibility of using an empirical shift correction to improve the results.

Table 3 summarizes the performance (Root Mean Square Deviations and absolute values of the largest and the smallest error) of all studied functionals with respect to the prediction of band positions and complexation-induced shifts. B3LYP is the best in reproduction of the maxima of spectral bands, yielding practically always the best result and with RMSD at least two times smaller than for other functionals. Likewise, the maximum error for B3LYP is also remarkably smaller. The LC-PBE is certainly the worst, and CAM-B3LYP and wB97XD give medium performance. For spectral shifts there is no clear winner; the LC-PBE is again the worst (generally overestimating the effect). The two other long-range-corrected functionals (CAM-B3LYP and wB97XD) perform reasonably well in estimating shifts of the absorption maximum (and of the 0–0 line); B3LYP seems relatively well suited for calculations of the shifts in emission spectra.

The results suggest that the long-range-corrected functionals does not improve results for ketocyanine dyes, instead, overestimating transition energies, they degrade the agreement with the experiment. Such behavior is not uncommon [6,10] and the effect of long-range corrections on $\pi \rightarrow \pi^*$ transitions for given class of compounds is difficult to predict without test calculations. As the HOMO and LUMO orbitals in ketocyanine dyes (especially in dyes B and C) occupy similar regions of space, the charge transfer upon

Table 3
Performance of tested functionals in prediction of absorption and emission maxima and spectral shifts for ketocyanine dyes. In each data category the best result is shown in boldface and the worst in italics.

Performance of the functional	B3LYP		CAM-B3LYP		LC-PBE		wB97XD	
	Abs.	Em.	Abs.	Em.	Abs.	Em.	Abs.	Em.
Positions of the maxima								
RMSD	**913**	**670**	2068	2700	*4550*	*4194*	2394	3024
$\|err_{max}\|$	**1661**	**1495**	2979	4112	*5432*	*5245*	3666	4235
$\|err_{min}\|$	**48**	**4**	1014	397	*2753*	*2745*	1312	1512
Best results	**16**	**17**	1	0	0	0	0	0
Worst results	0	0	0	0	*17*	*17*	0	0
Best res. – worst res.	**16**	**17**	1	0	*−17*	*−17*	0	0
Shifts								
RMSD	897	**371**	508	884	*1341*	*982*	**495**	807
$\|err_{max}\|$	1479	**787**	**953**	*2553*	*2199*	1888	1051	1546
$\|err_{min}\|$	*278*	53	91	*78*	12	**23**	**3**	29
Best results	*1*	**7**	3	*1*	2	2	**6**	2
Worst results	4	3	**0**	2	*7*	5	1	2
Best res. – worst res.	−3	**4**	3	−1	*−5*	*−3*	**5**	0

excitation is not large enough to require long-range corrections for proper reproduction of the transition energy.

4. Conclusions

We studied quantum-chemically the complexation-induced shifts in absorption or emission spectra of ketocyanine dyes interacting with metal ions in two common solvents. Four density functionals were used in DFT/TDDFT calculations. Features of simulated spectra were compared with available experimental data.

Relative strength of dye–cation interaction for different cations and solvents is easily rationalized by simple electrostatics and increases with increasing ion charge, decreasing ion radius and decreasing dielectric permittivity of the solvent. Binding of the ion is in all cases stronger in the excited rather than in the ground state of the dye, which may be attributed to increased dipole moment. The largest enhancement of the interaction strength in excited state is obtained in CAM-B3LYP calculations.

Observable transitions for all dyes and dye-cation complexes in acetonitrile and acetone are the lowest singlet transitions of HOMO → LUMO origin. Absorption or emission bands appear at the highest energies for dye A complexes and at the lowest for dye C; spectral shifts increase from Na^+ to Mg^{2+} in accordance with predicted changes in HOMO–LUMO separation and dye–ion interaction strength.

The best reproduction of the absorption and emission maxima is obtained for B3LYP; long-range-corrected functionals overestimate the energies, with LC-PBE being the worst. LC-PBE is also the worst performing in spectral shifts reproduction. wB97XD and CAM-B3LYP perform well for the absorption and the 0–0 line shifts and B3LYP yields reasonable accuracy for the changes in emission. The overestimate of the shifts obtained from wB97XD or CAM-B3LYP calculations seems to be systematic.

Presented results provide information about the performance of selected DFT functionals in the studies of spectral effects of ion complexation by ketocyanine dyes and therefore could help in proper choice of methodology for investigations of similar systems.

Acknowledgment

The equipment used in calculations was purchased with the financial support from the European Regional Development Fund in the framework of the Polish Innovation Economy Operational Program (Contract no. POIG.02.01.00-12-023/08).

Appendix A. Supplementary material

Supplementary material associated with this article can be found, in the online version, at doi:10.1016/j.comptc.2011.06.009.

References

[1] J.K. Basu, M. Shannigrahi, S. Bagchi, J. Phys. Chem. A 111 (2007) 7066.
[2] N. Ray, J.K. Basu, M. Shannigrahi, S. Bagchi, Chem. Phys. Lett. 404 (2005) 63.
[3] J.K. Basu, M. Shannigrahi, S. Bagchi, Chem. Phys. Lett. 431 (2006) 278.
[4] J.K. Basu, M. Shannigrahi, S. Bagchi, J. Phys. Chem. A 110 (2006) 2051.
[5] J.K. Basu, M. Shannigrahi, S. Bagchi, Chem. Phys. Lett. 441 (2007) 336.
[6] D. Jacquemin, E.A. Perpète, G. Scalmani, M.J. Frisch, R. Kobayashi, C. Adamo, J. Chem. Phys. 126 (2007) 144105.
[7] D. Jacquemin, E.A. Perpète, O.A. Vydrov, G.E. Scuseria, C. Adamo, J. Chem. Phys. 127 (2007) 094102.
[8] B.M. Wong, J.G. Cordaro, J. Chem. Phys. 129 (2008) 214703.
[9] D. Jacquemin, E.A. Perpète, G.E. Scuseria, I. Ciofini, C. Adamo, J. Chem. Theory Comput. 4 (2008) 123.
[10] D. Jacquemin, E.A. Perpète, I. Ciofini, C. Adamo, Theor. Chem. Acc. 128 (2011) 127.
[11] J. Ren, S. Meng, Ch.E. Lekka, E. Kaxiras, J. Phys. Chem. B 112 (2008) 1845.
[12] Ch.E. Lekka, J. Ren, S. Meng, E. Kaxiras, J. Phys. Chem. B 113 (2009) 6478.
[13] K. Fujimoto, W. Yang, J. Chem. Phys. 129 (2008) 054102.
[14] A. Berlin, C. Risko, M.A. Ratner, J. Phys. Chem. A 112 (2008) 4202.
[15] A. Tilocca, E. Fois, J. Phys. Chem. C 113 (2009) 8683.
[16] C.M. Choi, J.H. Lee, Y.H. Choi, H.J. Kim, N.J. Kim, J. Heo, J. Phys. Chem. A 114 (2010) 11167.
[17] A. Eilmes, J. Mol. Struct. THEOCHEM 915 (2009) 141.
[18] S.K. Sardar, K. Srikanth, S. Bagchi, J. Phys. Chem. A 114 (2010) 10388.
[19] A. Eilmes, Theor. Chem. Acc. 127 (2010) 743.
[20] M.J. Frisch, G.W. Trucks, H.B. Schlegel, G.E. Scuseria, M.A. Robb, J.R. Cheeseman, G. Scalmani, V. Barone, B. Mennucci, G.A. Petersson, H. Nakatsuji, M. Caricato, X. Li, H.P. Hratchian, A.F. Izmaylov, J. Bloino, G. Zheng, J.L. Sonnenberg, M. Hada, M. Ehara, K. Toyota, R. Fukuda, J. Hasegawa, M. Ishida, T. Nakajima, Y. Honda, O. Kitao, H. Nakai, T. Vreven, J.A. Montgomery, Jr., J.E. Peralta, F. Ogliaro, M. Bearpark, J.J. Heyd, E. Brothers, K.N. Kudin, V.N. Staroverov, R. Kobayashi, J. Normand, K. Raghavachari, A. Rendell, J.C. Burant, S.S. Iyengar, J. Tomasi, M. Cossi, N. Rega, J.M. Millam, M. Klene, J.E. Knox, J.B. Cross, V. Bakken, C. Adamo, J. Jaramillo, R. Gomperts, R.E. Stratmann, O. Yazyev, A.J. Austin, R. Cammi, C. Pomelli, J.W. Ochterski, R.L. Martin, K. Morokuma, V.G. Zakrzewski, G.A. Voth, P. Salvador, J.J. Dannenberg, S. Dapprich, A.D. Daniels, Ö. Farkas, J.B. Foresman, J.V. Ortiz, J. Cioslowski, D.J. Fox, Gaussian 09, Revision A.02, Gaussian, Inc., Wallingford CT, 2009.
[21] T. Yanai, D. Tew, N. Handy, Chem. Phys. Lett. 393 (2004) 51.
[22] H. Ilkura, T. Tsuneda, T. Yanai, K. Hirao, J. Chem. Phys. 115 (2001) 3540.
[23] J.-D. Chai, M. Head-Gordon, Phys. Chem. Chem. Phys. 10 (2008) 6615.
[24] A. Eilmes, P. Kubisiak, J. Phys. Chem. A 114 (2010) 973.
[25] F. Santoro, R. Improta, A. Lami, J. Bloino, V. Barone, J. Chem. Phys. 126 (2007) 084509.
[26] V. Barone, J. Bloino, M. Biczysko, F. Santoro, J. Chem. Theory. Comput. 5 (2009) 540.
[27] M. Cossi, V. Barone, J. Chem. Phys. 115 (2001) 4708.
[28] R. Cammi, F.J. Olivares del Valle, J. Tomasi, Chem. Phys. 122 (1988) 63.